Monte-Carlo simulation of electron conductance and magnetoresistance in magnetic polaron systems

J.-M. Liu[a)]
Laboratory of Solid State Microstructures, Nanjing University, Nanjing 210093, China and International Center for Materials Physics, Chinese Academy of Sciences, Shenyang, China

X. H. Zhou, X. Y. Chen, Z. G. Liu, Y. W. Du, and N. B. Ming
Laboratory of Solid State Microstructures, Nanjing University, Nanjing 210093, China

(Received 24 June 2002; accepted 18 September 2002)

The electron conductance and magnetoresistive effect in phase-separation-induced single-carrier magnetic polaron systems is studied by Monte-Carlo simulation. The simulation reveals the co-occurrence of ferromagnetic transition and insulating metallic transition as a function of temperature. The resistivity above the Curie point can be explained by the small-polaron mechanism and variable-range-hopping picture, while the resistivity far below the Curie point shows the contribution of two-magnon scattering. The electron tunneling behavior is confirmed by the nonlinear $I-V$ behaviors and the as-induced magnetoresistance is discussed. © *2002 American Institute of Physics.* [DOI: 10.1063/1.1520702]

The colossal magnetoresistance (CMR) discovered in perovskite manganites has been receiving increasing interests because of its potential applications. The most prominent feature with this effect is the co-occurrence of ferromagnetic (FM) transition and insulator–metal (I–M) transition with decreasing temperature T. A quite successful theory to explain the co-occurred transitions is the double-exchange model.[1] However, it was evidenced that the antiferromagnetic (AFM) superexchange represents an intrinsic background in the manganites and the competition between the AFM superexchange and the FM double exchange is mainly responsible for the fascinating electric and magnetic phenomena. A fundamental problem is that any homogeneous ground state at partial filling of the conduction band may be unstable against a phase separation.[2,3] The phase-separated ground state is composed of magnetic polarons that are FM droplets surrounding charge carriers in the AFM background. If the polarons cannot move for large effective mass and/or disorder, the FM–AFM phase-separated structure represents the ground state.

For a pure magnetic polaron system, it is assumed that each polaronic droplet contains one charge carrier confined in a potential well of ferromagnetically ordered local spins.[4,5] Consequently, the conduction is thought to be mainly attributed to the electron tunneling among the isolated droplets. With decreasing T, the droplets develop both in number and volume so that a percolation threshold is reached, resulting in the I–M and FM transitions at T_m and T_c, simultaneously, i.e., $T_m \sim T_c$. This picture above $T_m - T_c$ was described by a classical droplet model that applies as the carrier concentration is much smaller than the percolation threshold.[6–8] For $T < T_m$, the droplet model is no longer applicable and the long-range ordering should be considered.

However, it needs to be addressed that the physical mechanisms underlying the phase separation in real CMR materials are much more complicated than the present magnetic polaron picture. Experimentally it is demonstrated that at $T < T_m$ the structure consists of FM and metallic clusters of a few to tens nanometers in size coexisted with insulating matrix.[9–11] Each metallic cluster contains far more than one carrier. The physics may be understood from two aspects. On one hand, in terms of the polaron picture, the percolation transition at a high volume fraction of the polarons results in aggregation of polarons, i.e., forming the metallic clusters. On the other hand, there are additional ordering interactions such as orbital ordering and charge ordering needed to be taken into account to have a full-scale understanding of the phase separation.[11–13] Therefore, the magnetic polaron picture only represents one of the physical mechanisms responsible for the phase separation in real CMR systems. In this letter, we focus on a pure magnetic polaron system and perform a Monte-Carlo (MC) simulation on the electron conductance over the whole temperature range to demonstrate the co-occurrence of the two transitions.

The MC simulation is performed by starting from the droplet model for a squared lattice. Consider an insulating AFM lattice of volume V_s under an electric field E. There are N magnetic polarons (droplets) distributed in the sample with their spatial density $n = N/V_s$. The system energy in the framework of mean-field approach can be written as[6,8]

$$H = t(\pi d/a)^2 + J_{\mathrm{AF}} S^2 (4\pi/3)(a/d)^3, \tag{1}$$

where t is the bandwidth, d is the intersite distance, a is the droplet radius, J_{AF} is the AFM Heisenberg exchange, and S is the local spin moment inside droplet. It is assumed that one magnetic polaron at the ground state contains one electron (this assumption can be relaxed without changing the main conclusion). Assuming the energy for a droplet with m electrons is $K(m)$, one has[8]

$$K(0) \sim 0, \quad K(1) \sim t(d/a)^2, \quad K(2) \sim 2K(1) + U \tag{2}$$

with U being the interaction energy of the two electrons. Therefore, the creation of two electron droplets has to overcome an energy barrier of $A \equiv K(2) - 2K(1) \sim U$. Energy U is mainly attributed to the Coulomb repulsion between two electrons, so $A \equiv U \sim e^2/\epsilon a$ with ϵ being the static dielectric constant. Thus, three types of droplets $m = 0$, 1, and 2, exist

a)Electronic mail: liujm@nju.edu.cn

in the system. A droplet with more than two electrons is considered to be unstable due to the strong Coulomb repulsion. The four elementary sequences ($i=1,2,3,4$) for electron tunneling proposed earlier produce a current density j in the linear regime[6,8]

$$j=j_1+j_2+j_3+j_4,$$
$$j_{1,2,3,4}=en_{1,2,3,4}\left\langle \sum v^i_{1,2,3,4}\right\rangle, \tag{3}$$

where j_i is the current density from sequence i, e is the electron charge, $v^i_{1,2,3,4}$ is the electron drift velocity, $n_{1,2}=N_{1,2}/V_s$ and $\langle\cdots\rangle$ stands for statistical and time average. In the defined spatial coordinates, we have

$$\left\langle \sum_i v^i_{1,2,3,4}\right\rangle=\left\langle \sum_i \frac{r^i\cos\theta^i}{\tau_{1,2,3,4}(r^i,\theta^i)}\right\rangle, \tag{4}$$

where r^i and θ^i are the electron tunneling length (the distance between the droplets) and the angle between E and the direction of motion, respectively; τ_i is the characteristic time for the tunneling processes. The times for the tunneling modes $i=1$ and 2 are written as[8]

$$\tau_{1,2}(r,\theta)=\omega_0^{-1}\exp\left(\frac{r}{l}\pm\frac{A}{2kT}-\frac{eEr\cos\theta}{kT}\right) \tag{5}$$

with l and ω_0 the characteristic tunneling length and magnon frequency, k is the Boltzmann constant. The tunneling is spin dependent and the static magnetic energy besides the Coulomb interaction and static electric energy should be taken into account too, thus Eq. (5) becomes

$$\tau_{1,2}(r,\theta)=\omega_0^{-1}\exp\left(\frac{r}{l}\pm\frac{A}{2kT}-\frac{eEr\cos\theta}{kT}-\frac{T_{mn}\cdot S_mS_n\cos\phi}{kT}-\frac{g\mu_BS_mH\cos\vartheta}{kT}\right), \tag{6}$$

where T_{mn} is the energy factor for the spin-dependent tunneling, subscripts (m,n) stand for two neighboring sites, ϕ is the angle between spins S_m and S_n, g is the spin number, μ_B is the Bohr magnetron, and ϑ is the angle between spin S_m and applied magnetic field H. For sequences (3) and (4), the corresponding characteristic times are

$$\tau_{3,4}(r,\theta)=\omega_0^{-1}\exp\left(\frac{r}{l}-\frac{eEr\cos\theta}{kT}-\frac{T_{mn}\cdot S_mS_n\cos\phi}{kT}-\frac{g\mu_BS_mH\cos\vartheta}{kT}\right). \tag{7}$$

The number density n for droplets (the interdroplet distance r) is dependent of the system magnetization M. This dependence is assumed to be linear and approached by $n=M/M_s$ with M_s the saturated magnetization. The magnetic behavior is described by the Hamiltonian

$$H_M=-J_{\mathrm{FM}}\sum_{\langle m,n\rangle}S_m\cdot S_n-J_{\mathrm{AF}}\sum_{[m,n]}S_m\cdot S_n, \tag{8}$$

where J_{FM} and J_{AF} are the energy terms for FM and AFM exchanges, and $\langle\cdots\rangle$ and $[\cdots]$ mean summation over the nearest and next-nearest spin pairs once, respectively.

The simulation starts from a two-dimensional (2D) $L\times L$ squared lattice with a periodic boundary condition applied. A simulation in a three-dimensional $L\times L\times L$ cubic lattice is performed also to compare with the results in the 2D case. And there is no substantial difference between them. Each site of the lattice is imposed on a spin of moment S in a random order of spin-up or spin-down. The intersite distance d is taken and the average droplet radius a is $a\sim d(t/J_{\mathrm{AF}}S^2)^{1/5}$. The simulation is performed in one cycle by the following steps. (1) The standard *Metropolis* algorithm is employed to obtain the statistically averaged magnetization M at a given T, and then the number density of droplets n ($0<n\leqslant 1$) is calculated. The mcs number for the statistics is 10^5. (2) $nL^2(nL^3)$ droplets are generated randomly in the lattice of droplet density n. (3) Consider stochastic tunneling of electron between two droplets by employing the standard Metropolis algorithm. (4) Under given E and H, the system conductivity is evaluated by Eqs. (3), (4), (6), and (7) through spatial summation over the whole lattice.

TABLE I. System parameters chosen for the simulation.

Parameter	Value	Parameter	Value
e (C)	1.602×10^{-19}	K (J/K)	1.38×10^{-23}
μ_B (J/T)	9.27×10^{-24}	g	19
d (nm)	0.50	ϵ	20
t (J)	1.0×10^{-23}	J_{FM} (J)	5.0×10^{-21}
J_{AF} (J)	1.0×10^{-21}	S	3/2
l (nm)	1.0	ω_0 (Hz)	1.0×10^{8}
T_{mn} (J)	5.0×10^{-21}	L	64
E (V/m)	1.0×10^{5}		

In our simulation, the system parameters we choose are listed in Table I. In Fig. 1 the simulated resistivity ρ and magnetization M as a function of T under various fields are plotted. First, the insulating behavior over high T and metallic one over low T are revealed with a clear I–M transition at $T_m\sim400$ K. Correspondingly, a FM transition is observed at T_c. The one-to-one correspondence between T_c and T_m is shown, demonstrating the cooccurrence of FM and I–M transitions.

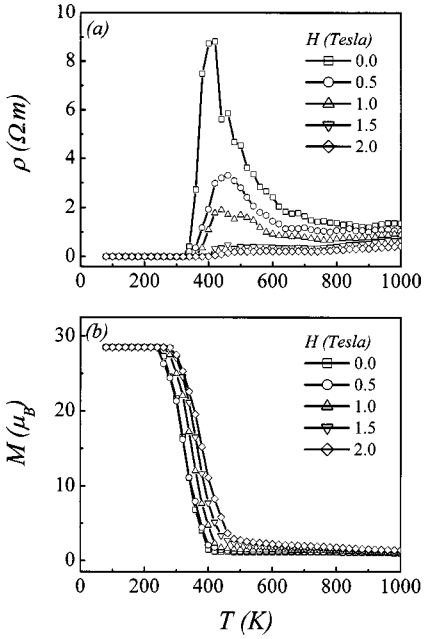

FIG. 1. (a) System resistivity ρ and (b) magnetization M as a function of temperature T under various magnetic fields H (T) as indicated numerically.

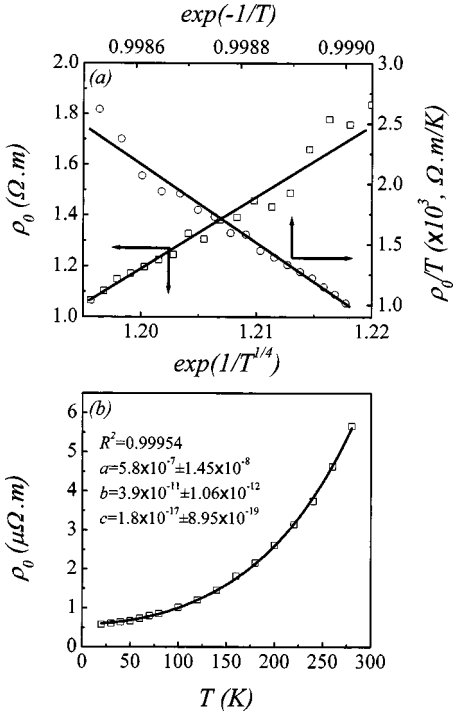

FIG. 2. Fitting of the simulated zero-field resistivity ρ (a) at $T \gg T_m$ and (b) at $T \ll T_m$ by the variable-range-hopping conductivity and small-polaron conductivity.

The magnetic polaron model[8] predicts that the conductivity at $T \gg T_m$ can be described by the small polaron picture $\rho_0/T = \rho_{i0} \exp(-Q/kT)$, where ρ_{i0} is the prefactor and Q the activation energy, and the variable-range-hopping (VRH) picture $\rho_0 = \rho_{i0} \exp(T_0/T)^{1/4}$, where T_0 is the characteristic temperature, to fit the data. In Fig. 2(a) one plots the resistivity data at $T \gg T_m$ in terms of the two mechanisms. It seems that both mechanisms work roughly well, with the small polaron mode better than the VRH mode. This proves the magnetic polaron picture as a possible and acceptable model for the electron tunneling far above T_m.

As for the conduction at $T \ll T_m$, it was demonstrated recently that the carrier charges are still polaronic, with the itinerant electrons contributing to the low T conduction.[14,15] Therefore, the low T resistivity should contain $T^{4.5}$ component besides the zero-point resistivity and electron–electron scattering (T^2 component). We plot the data at extra-low temperature in Fig. 2(b) and use $\rho_0 = a + bT^2 + cT^{4.5}$, where a, b, and c are the temperature constants, to fit the data. Since $c \gg b^{2.25}$, the contribution of the two-magnon scattering is significant, indicating that the carrier charges are indeed polaronic, although the electron–electron scattering cannot be neglected. The polaronic nature of the carriers in the FM state at very low T reflects the essential role of magnetic polaron conduction.

Although the electron tunneling is responsible for the conduction, its role at $T < T_m$ should be confirmed. We simulate the $I-V$ relationships at $T > T_m$ and $T < T_m$. As $T > T_m$, it is quite clear that the $I-V$ curves are nonlinear over the whole range of E covered here, demonstrating the dominance of the tunneling conduction. As for $T < T_m$, the conduction behavior at high E is Ω type, producing a linear $I-V$ relation. This is also confirmed with our simulation. Nevertheless, the nonlinear $I-V$ behavior can be clearly identified when E is low, which indicates the dominance of tunneling conduction under low E. This result is intrinsically consistent with the picture of polaronic carrier charges in the FM state at low T.

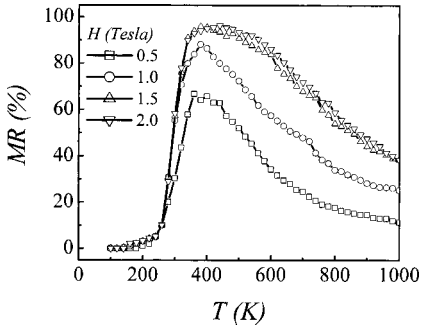

FIG. 3. Magnetoresistance MR as a function of temperature T under various magnetic fields H (T) as indicated numerically.

Finally, the evaluated magnetoresistance $\mathrm{MR} = [\rho(0) - \rho(H)]/\rho(0)$ under various H is plotted in Fig. 3. The maximum MR is achieved around $T \sim T_c \sim T_m$. As for the MR effect far from the transition point, the simulated MR becomes quite small as $T \ll T_c$. This is understandable because almost all spins in the lattice are well aligned and no further spin-dependent tunneling induced MR effect can be activated.

In conclusion, a Monte-Carlo simulation on the conduction and magnetoresistance in pure magnetic polaron systems has been presented. The well-established I–M transition accompanied with FM transition with decreasing temperature has been reproduced in the simulation. The conduction behaviors over high and low temperatures can be described by the magnetic polaron model and the present simulation allows us to argue the essential role of magnetic polaron mechanism in determining the magnetoresistance in manganites and other transition metal FM systems.

This work was supported by the Natural Science Foundation of China through the innovative group project and Project No. 10074028.

[1] C. Zener, Phys. Rev. **82**, 403 (1951).
[2] J. M. D. Coey, M. Viret, and S. von Molnar, Adv. Phys. **48**, 167 (1999).
[3] J. A. Verges, V. Martin-Mayor, and L. Brey, Phys. Rev. Lett. **88**, 136401 (2002).
[4] P. G. de Gennes, Phys. Rev. **118**, 141 (1960).
[5] E. L. Nagaev, Sov. Phys. Usp. **166**, 833 (1996).
[6] M. Yu. Kagan, D. I. Khomskii, and M. V. Mostovoy, Eur. Phys. J. B **12**, 217 (1999).
[7] M. Hennion, F. Moussa, G. Biotteau, J. Rodriguez-Carvajal, L. Pinsard, and A. Revcolevschi, Phys. Rev. Lett. **81**, 1957 (1998).
[8] A. L. Rakhmanov, K. I. Kugel, Ya. M. Blanter, and M. Yu. Kagan, Phys. Rev. B **63**, 174424 (2001).
[9] M. Uehara, S. Mori, C. H. Chen, and S.-W. Cheong, Nature (London) **399**, 560 (1999).
[10] M. Fäkh, S. Freisem, A. A. Menovsky, Y. Tomioka, J. Aarts, and J. A. Mydosh, Science **285**, 1540 (1999).
[11] For more references, refer to E. Dagotto, T. Hotta, and A Moreo, Phys. Rep. **344**, 1 (2001).
[12] H. Y. Hwang, S.-W. Cheong, P. G. Radaelli, M. Marezio, and B. Batlogg, Phys. Rev. Lett. **75**, 914 (1995).
[13] H. Kawano, R. Kajimoto, H. Yoshizawa, Y. Tomioka, H. Kuwahara, and Y. Tokura, Phys. Rev. Lett. **78**, 4253 (1997).
[14] G. M. Zhao, Phys. Rev. B **62**, 11639 (2000).
[15] G. M. Zhao, Y. S. Wang, D. J. Kang, W. Prellier, M. Rajeswari, H. Keller, T. Venkatesan, and C. W. Chu, Phys. Rev. B **62**, R11949 (2000).